A Multi-Physics Study of the Wave Propagation Problem in Open Cell Polyurethane Foams

M. Brennan[1], M. Dossi[1], M. Moesen[1]
1. Huntsman Polyurethanes, Everslaan 45, 3078 Everberg, Belgium.

Abstract

Flexible and semi-rigid polyurethane (PU) foams are widely used as noise and vibration damping materials. Their porous random microstructure is composed of a visco-elastic frame structure with an interstitial fluid, normally air, filling the voids. The viscoelasticity of the foams is due to the polymer morphology in the foam skeleton structure. PU foams are often partially-open foams in which cell faces are partially covered by thin membranes, which could influence the viscous-thermal foam dissipation. The energy transport is carried both through the air-borne flow in the pores as well as through the solid frame structure-borne vibration transmission. The mechanical and acoustic waves are strongly coupled; for this reason, to study the wave propagation in porous foams, a solution of fluid-structure interaction problem is required.

In this work, COMSOL Multiphysics® Modeling Software is used to study the wave propagation problem in porous foams. Computational fluid dynamic is used to predict foam permeability k through a 2D axial-symmetric reference model and a Kelvin foam model with regular cell hole sizes. The coupling between air- and structure-borne wave propagation is analysed to study the effect of cell face membranes on wave propagation through open cell PU foam.

Introduction

Flexible and semi-rigid polyurethane (PU) foams are widely used as noise and vibration damping materials. PU flexible foam chemistry is a urethane reaction of isocyanate and polyol to form a soft-like polymer and a urea reaction of isocyanate with water to provide the blowing agent, through CO_2, which is released during the reaction [1]. The former reaction gives the foam its flexibility, strength and vibration damping properties, while the latter leads to the cellular microstructure and urea groups that phase separate into hard segments and contribute to the load bearing properties of the foam. The PU foam has a porous random microstructure, composed of a visco-elastic frame structure with an interstitial fluid, i.e. air, filling the voids. PU foams are often partially-open foams, in which cell faces are partially covered by thin membranes (see Figure 1), which could influence the viscous-thermal dissipation in foams [2] as well as the elastic properties [3].

The energy transport is carried both through the air-borne flow in the pores as well as through the solid frame structure-borne vibration transmission. Several methods have been developed to model acoustic porous materials through an equivalent fluid models, in which the acoustic properties depend on the effective density and the effective bulk modulus of the fluid. Some of the widely-used phenomenological model are: Zwikker and Kosten's analytical model to study the case of a cylindrical pore [4], Johnson–Champoux–Allard–Lafarge's (JCAL) model which introduces the concept of a viscous and thermal characteristic lengths to model the porous material behaviour in all frequency range [5] and the relaxation-matched model of propagation through porous media proposed by Wilson [6]. Conventionally, an idealized unit cell representing the micro-structure of the porous material is created, often based on geometrical parameters obtained from micro-structure characterization techniques [3, 7]. The non-acoustical parameters are then linked to the unit cell through a phenomenological model using empirical relations or calculated numerically by solving a steady Stokes problem and a thermal conduction problem into the representing unit cell [3]. In [8], the author showed how the cellular micro-structure, in particular cell anisotropy and pore size connections, influence sound absorption in open cell foams with a rigid frame.

However, the equivalent fluid models do not consider the structure vibrations and therefore they are not able to completely describe the coupled mechanical and acoustic wave propagation in the PU open cell foam. Moreover, the foam microstructure is often polydisperse and characterized by partially-open cells, as shown in Figure 1. Therefore, the wave propagation could be influenced by the local visco-thermal dissipations of the fluid but also by the vibration of the pore membranes [9]; the Fluid-Structure Interaction (FSI) can then not be neglected. One of the widely-used coupling theories is probably Biot's model [10], which links the macroscopic fluid and solid displacement fields with the effective parameters. Recently, a study of the sound propagation problem in porous materials by adopting the framework of the

computational homogenization method has been proposed [7].

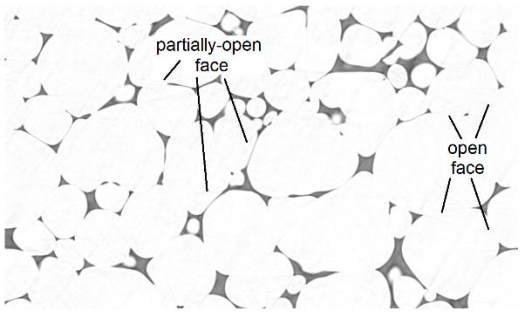

Figure 1. 2D image of of X-ray tomography data of a flexible PU foam.

In this work, COMSOL Multiphysics® Modeling Software is used to study the wave propagation problem in porous foams; CFD, Acoustics and Structural Mechanics modules are used to model the air-borne transmission, the structure-borne one, and their multi-physics coupling. Two types of unit cell have been considered: a 2D axial-symmetric reference model, in which the cell-face is perpendicular to the flow, and a 3D Kelvin model [11], characterized by a space filling with the least surface energy. An oscillating pressure gradient is applied to the unit cells to study the wave propagation phenomena. In particular, different cell opening ratios are considered to study the local effect of pore membrane vibrations. Wilson's relaxation-matched model of propagation through porous media is used to link the fluid micro-structure interaction response to some macroscopic properties, e.g. dynamical permeability $\boldsymbol{k}$ and tortuosity ∞.

The present paper is organized as follows: in the next sessions the formulation of the fluid-structure interaction problem and the mathematical model of dynamic viscous permeability in open cell foams are described. Then, 2D and 3D numerical examples are discussed to show how COMSOL Multiphysics® has been used to study the wave propagation problem in open cell polyurethane foams. Final remarks are given in last section.

Formulation of the fluid-structure interaction problem

The FSI combines fluid flow with solid mechanics to capture the interaction between the fluid and the solid structure. In COMSOL, a Solid Mechanics interface and a Single-Phase Flow interface model the solid and the fluid, respectively [12].

The fluid flow is described by the Navier-Stokes equations, which provide a solution for the velocity field, $\boldsymbol{v}$. Assuming that the inertial term in the Navier-Stokes equations can be neglected due to the small geometrical scale of the foam structure and to the small velocity of air through open cells, the equations for conservation of momentum and the continuity equation for conservation of mass, governing the non-stationary evolution of an incompressible flow, are:

$$\rho_f \frac{\partial \boldsymbol{v}}{\partial t} = \nabla \cdot [-p\boldsymbol{I} + \mu(\nabla \boldsymbol{v} + \nabla \boldsymbol{v}^T)] + \boldsymbol{F}_f \qquad (1)$$

$$\rho_f \nabla \cdot \boldsymbol{v} = 0. \qquad (2)$$

In Eq. (1-2): ρ_f and μ are the density and the dynamic viscosity of the air, respectively, p is the fluid pressure, t is the time, $\boldsymbol{F}_f$ is the external force applied to the fluid**,** $\boldsymbol{I}$ is the identity matrix, ∇ and $\nabla \cdot$ are the gradient and divergence operators.

The linear elasto-dynamic problem for the solid domain is governed by the following set of equations:

$$\rho_s \frac{\partial^2 \boldsymbol{u}}{\partial t^2} - \nabla \cdot \boldsymbol{\sigma} = \boldsymbol{F}_s. \qquad (3)$$

In Eq. (3): ρ_s is the solid density, $\boldsymbol{u}$ is the solid displacement, $\boldsymbol{F}_s$ is the body force applied to the solid. $\boldsymbol{\sigma} = J^{-1}\boldsymbol{F}\boldsymbol{S}\boldsymbol{F}^T$ is the Cauchy stress tensor, being $\boldsymbol{F}$ the deformation tensor, J its determinant and $\boldsymbol{S}$ the second Piola-Kirchhoff stress tensor [13]. The constitutive behavior of the solid is then described as:

$$\boldsymbol{S} = \frac{1}{2}\boldsymbol{C}\colon[\nabla \boldsymbol{u}^T + \nabla \boldsymbol{u} + \nabla \boldsymbol{u}^T \nabla \boldsymbol{u}], \qquad (4)$$

where $\boldsymbol{C}$ is the Green deformation tensor and : stands for the double-dot tensor product. In Eq. (3-4), the absence of any inelastic term has been assumed. To a complete formulation of the problem into the fluid and solid domains, the Navier-Stoke and elasto-dynamic governing equations have to be solved together with the appropriate boundary conditions.

The FSI coupling appears on the boundaries between the fluid and the solid, and it defines how structural displacements affect the fluid velocity and the fluid load on the solid domain, respectively:

$$\boldsymbol{v} = \frac{\partial \boldsymbol{u}}{\partial t} \qquad (5)$$

$$\boldsymbol{\sigma} \cdot \boldsymbol{n} = [-p\boldsymbol{I} + \mu(\nabla \boldsymbol{v} + \nabla \boldsymbol{v}^T)] \cdot \boldsymbol{n}, \qquad (6)$$

where $\boldsymbol{n}$ is the outward normal to the boundary. The FSI interface uses an Arbitrary Lagrangian-Eulerian (ALE) method to combine the fluid flow formulated using an Eulerian description and a spatial frame with solid mechanics formulated using a Lagrangian description and a material, i.e. reference, frame [12].

Mathematical model of dynamic viscous permeability in open cell foams

To represent a sound wave at a particular frequency a one-direction sinusoidal pressure gradient is applied across the foam microstructure. Within a few cycles, the average velocity oscillates at the same frequency as the average pressure gradient, but it will be shifted by a phase angle φ with respect to the pressure gradient oscillation [8]. This is expressed mathematically as:

$$\nabla\langle p\rangle = \frac{i\langle P_0\rangle e^{iwt}}{l} \tag{7}$$

$$\nabla\langle v\rangle = -i\langle v_0\rangle e^{i(wt+\varphi)}, \tag{8}$$

where the brackets $\langle\ \ \rangle$ denote the volume average.

Darcy's law for porous materials defines the relationship between the average pressure gradient and the average velocity by means of a dynamic viscous permeability:

$$k(w) = -\mu\,\frac{\langle v\rangle}{\nabla\langle p\rangle} = \mu\,\frac{\langle v_0\rangle}{\frac{i\langle P_0\rangle}{l}}e^{i\varphi}. \tag{9}$$

The permeability can be decomposed into a real part and an imaginary part as follows:

$$k(w) = k' + ik'' = |k|cos(\varphi) + |k|sin(\varphi), \tag{10}$$

where the module of permeability assumes the following expression:

$$|k| = \mu\frac{\langle v_0\rangle}{\frac{\langle P_0\rangle}{l}}. \tag{11}$$

The frequency response of the real and imaginary parts of the permeability depends on the foam cell morphology. The static permeability is the permeability at the low frequency range and is defined as $k_0 = k(w \to 0)$. The flow resistivity is related to the static permeability by the relationship $\sigma_0 = \frac{\mu}{k_0}$. This is what is measured with an air flow resistivity experiment.

It is not necessary to solve the Stokes equations for each frequency for a given foam cell morphology. Indeed, using Wilson's model of sound propagation in a porous material [6] is possible to fit a number of permeability simulations in order to obtain the dynamical permeability in all frequency range, according to:

$$k(w) = \frac{\mu}{\alpha_\infty\rho_f iw}\left(1 - \sqrt{1 - \frac{iwk_0 2\alpha_\infty\rho_f}{\mu}}\right). \tag{12}$$

Wilson's model describes acoustic propagation in a porous material as a relaxation process. In a similar way to the interpretation of viscoelastic measurements, the relaxation times can be introduced to describe the flow relaxation processes involved in acoustic propagation. When a pressure gradient is applied across a porous medium, such relaxation time can be thought of as the time for the velocity field to establish equilibrium with the counteracting frictional forces.

So, for a given set of fluid physical properties, the fluid density ρ_f, the viscosity μ, and a set of topological parameters, the static viscous permeability k_0 and the tortuosity α_∞ are obtained from fitting simulation results and the frequency dependent flow of a given foam morphology are completely described.

Numerical example

2D reference model

The first example concerns a 2D axial-symmetric reference model of a single cell face of diameter $d = 1.22 \cdot 10^{-4}m$, similar to Gent and Rusch's one [14]. Although the simplicity of the example, i.e. 2D geometry and cell-face perpendicular to the flow, makes it difficult to relate the model parameters directly to the foam microstructural ones, such a qualitative model is a starting point for developing a fundamental understanding of the wave propagation into PU foams with near-circular face holes. Different opening ratios (0.1, 0.3, 0.5 and 0.7) are considered to study the effect of morphology, as shown in Figure 2. A one-direction sinusoidal pressure gradient $(0{,}1[Pa]\sin(wt), 0)$ is applied across the unit cell and no-slip boundary conditions, i.e. $\boldsymbol{v} = 0$, are imposed on the others walls.

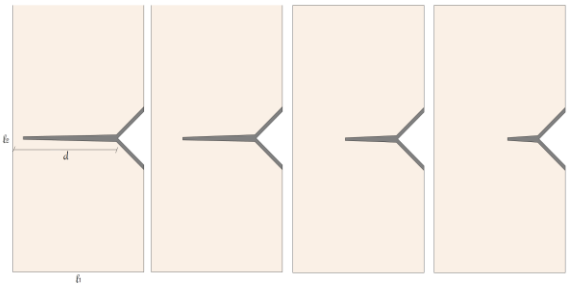

Figure 2. 2D axial-symmetric reference model of a single cell face of diameter *d* with different opening, 0.1*d*, 0.3*d*, 0.5*d*, 0.7*d*. The grey part represents the cellular micro-structure.

Firstly, the cellular micro-structure is assumed to be perfectly rigid, i.e. only air-borne wave propagation is studied. The air viscosity is assumed equal to $18 \cdot 10^{-6}\ Pa \cdot s$ and the air density equal to $1.29\,\frac{kg}{m^3}$. As

mentioned earlier, at low frequencies the average flow through the foam cell is in phase with the pressure gradient but, as the frequency increases, the average flow shifts phase with the pressure gradient tending to $\frac{\pi}{2}$, see Figure 3. The phase shift occurs faster at high opening ratio, see Figure 4.

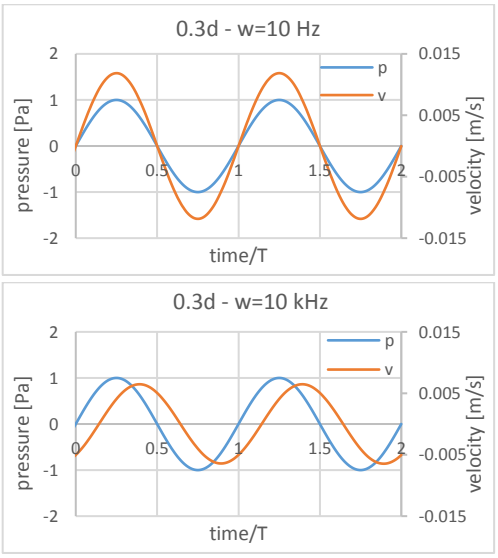

Figure 3. 2D axial-symmetric reference model of a single cell face with opening 0.3d. Increasing the frequency of the pressure gradient (10 Hz upper row, 10 kHz bottom row), the velocity amplitude decreases and phase angle increases.

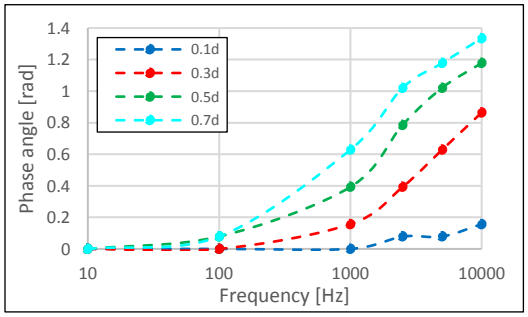

Figure 4. Comparison of air-borne wave propagation into 2D reference models in terms of phase angle depending of the pressure gradient frequency.

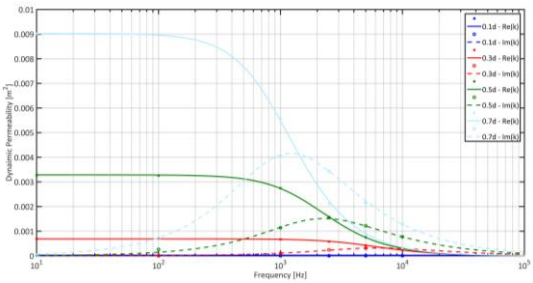

Figure 5. Comparison of air-borne wave propagation into 2D reference models in terms of real and imaginary dynamical permeability depending of the pressure gradient frequency. Points are the simulation results, curves are the fitting using Wilson's model.

Figure 5 shows the comparison of air-borne wave propagation in terms of real and imaginary parts of dynamical permeability. As the frequency of the pressure gradient tends to 0, the dynamic permeability tends to the static one, k_0. The results confirm the dependence of real and imaginary parts of the permeability by the cell morphology; indeed, increasing the cell opening, the static permeability increases [16, 17]. When w becomes large, the effect of viscosity dissipation becomes negligible and k tends to the tortuosity α_∞.

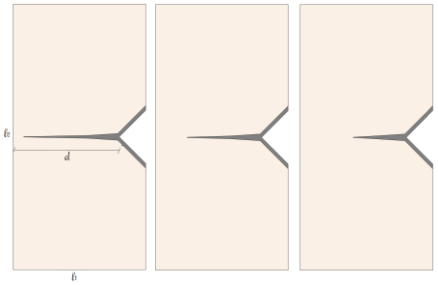

Figure 6. 2D axial-symmetric reference model of a single cell face of diameter d with different opening, 0.1d, 0.3d, 0.5d. The cell face is partially covered by a thin membrane.

Secondly, the cellular micro-structure is modelled as linear elastic material, with density $\rho_s = 1100 \frac{kg}{m^3}$, Young's modulus $E = 10^8\ Pa$ and Poisson's ratio $\nu = 0.45$. In this case, the structure thickness and the low value of the pressure gradient applied prevent the vibration of the cellular micro-structure. Hence, the wave propagation remains almost the same of the previous case, see Table 1.

Table 1. Static permeability values depending of opening ratio and type of physics involved.

	2D-air	**2D-FSI**	**2D-FSI with membrane**
$\mathbf{0.1}d$	$2.25\ 10^{-5}$	$2.16\ 10^{-5}$	$3.78\ 10^{-5}$
$\mathbf{0.3}d$	$6.84\ 10^{-4}$	$6.67\ 10^{-4}$	$1.09\ 10^{-3}$
$\mathbf{0.5}d$	$3.27\ 10^{-3}$	$3.23\ 10^{-3}$	$4.93\ 10^{-3}$
$\mathbf{0.7}d$	$8.97\ 10^{-3}$	$9.02\ 10^{-3}$	– –

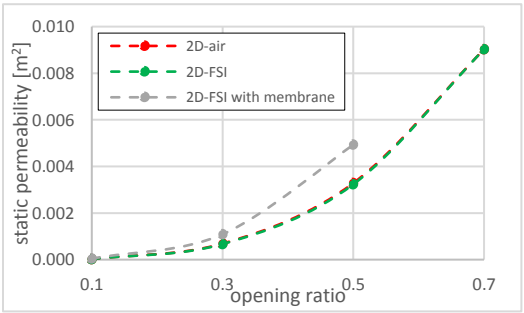

Figure 7. Comparison of air-borne (2D-air), structural-borne (2D-FSI) and structural-borne with membrane (2D-FSI with membrane) wave propagation into 2D reference models in terms of static permeability.

However, many acoustic foams are partially-open foams in which cell faces are partially covered by thin membranes. To consider the effect of such membranes, starting from the geometry with opening $0.7d$, new geometries are built, reducing the structure thickness as shown in Figure 6. In this case, the thin membrane bends and the effect is comparable to an increasing of cell opening; indeed, the airflow resistance decrease, i.e. the static permeability increases, see Figure 7. Such membrane effect disappears at high frequency because the solid-structure dissipation is governed by inertial dissipation, as shown in the Figure 8, which compares the wave propagation with opening $0.3d$ and $0.5d$ in the cases with and without the membrane.

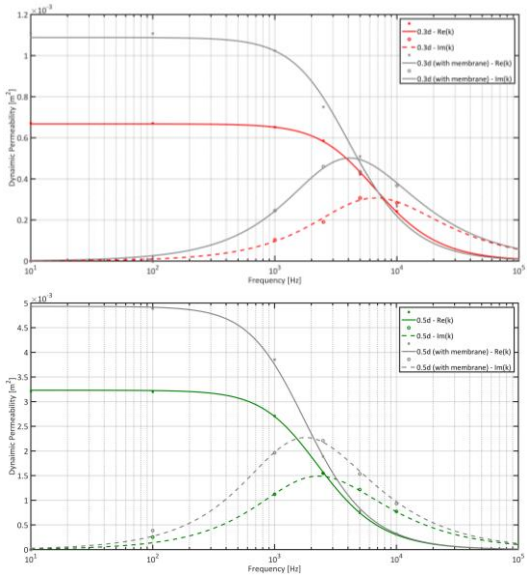

Figure 8. Comparison of structural-borne and structural-borne with membrane wave propagation into 2D reference models with opening $0.3d$ (upper row) and $0.5d$ (bottom row) in terms of dynamic permeability.

Kelvin cell model

In the second example, a Kelvin unit cell model is considered [11], which fully fills the space and nearly minimizes the surface energy; each cell is composed by six square and eight hexagonal faces, with all edge lengths being equal. The faces are covered by thin membranes with a circular opening in the center. Different opening ratios, defined as the area of the opening relative to the total face area, are consider (K5 (0.05 opening ratio), K10, K20 and K30), see Figure 9. An x-direction sinusoidal pressure gradient $(100[Pa]sin(wt),0,0)$ is prescribed. Same air and polymer properties of the previous example are considered. This 3D model has the limitation that all faces are assumed to contain equal holes. Readers can refer to [15] for a complete description of a method for creating computational foam micro-structures of ideal foams.

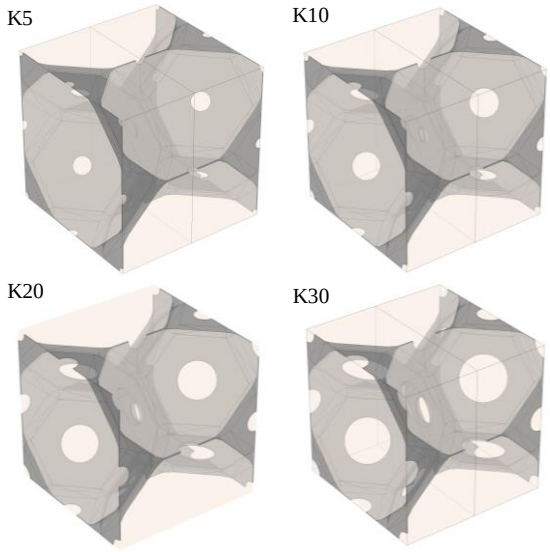

Figure 9. 3D Kelvin cell models characterized by opening ratios equal to 0.05 (K5), 0.1 (K10), 0.2 (K20), 0.3 (K30).

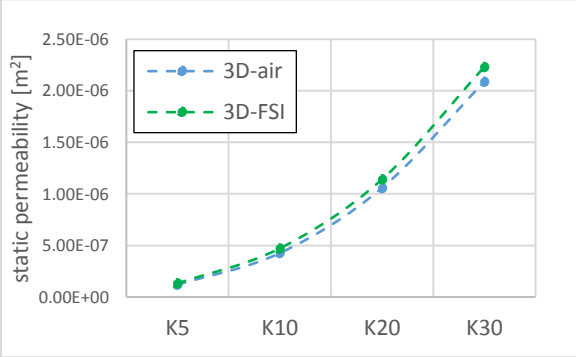

Figure 10. Comparison of air-borne (3D-air) and its coupled interaction with structural-borne (3D-FSI) wave propagation into 3D kelvin cells in terms of static permeability.

The 3D results confirm the same tendency of 2D one; indeed, according to [16, 17], the foam micro-structure with a higher opening ratio has a higher static permeability, see Figure 10. Again, when a fluid-structure interaction is considered, the fluid flow increases due to the bending of the membranes and consequently the static permeability increases. Figure 11 shows how such effect of the membranes decreases with increasing frequency.

Figure 12 shows the velocity streamlines at time of maximum pressure through foam microstructure of K5 and K30 at 10 Hz and 2500 Hz. Notice that in addition to the increase in flow, the streamlines also become less tortuous as the opening ratio of foam cell increases. Figure 12 quantifies also the von Mises stress on the cellular micro-structure; decreasing the opening ratio of the cell, the stress concentrations are

higher and are located along the membrane-structure connection. When the cell faces are more covered by membranes, the regions of the membrane close to the holes present higher displacement, because they are more free to bend, as quantified in Figure 13. This explains the membrane effect, equivalent to an increasing of cell opening, already shown in the 2D example.

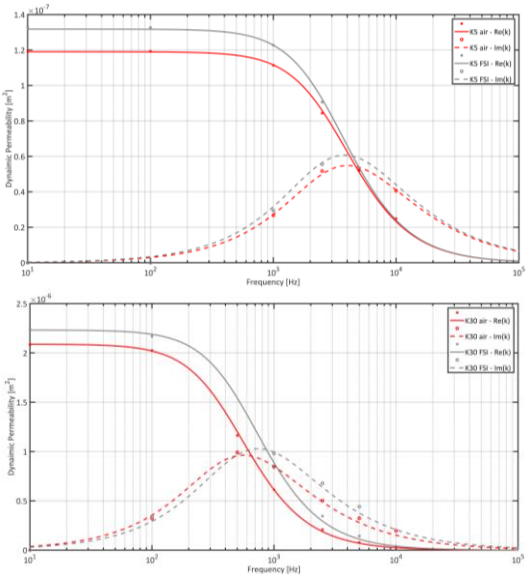

Figure 11. Comparison of air-borne (air) and its coupled interaction with structural-borne (FSI) wave propagation into 3D kelvin cells with opening ratio 0.05 (K5, upper row) and 0.30 (K30, bottom row) in terms of dynamic permeability.

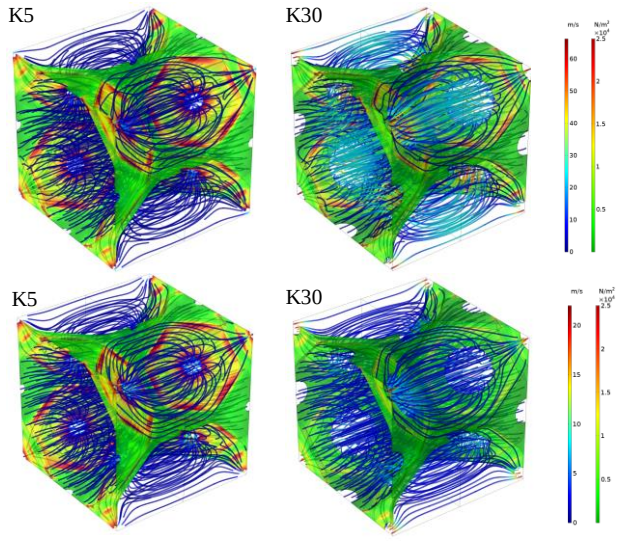

Figure 12. Velocity streamlines at time of maximum pressure through foam microstructure of K5 (left column) and K30 (right column). The von Mises stress are plotted on the cellular micro-structure. Two frequencies are considered: 10 Hz (upper row) and 2500 Hz (bottom row).

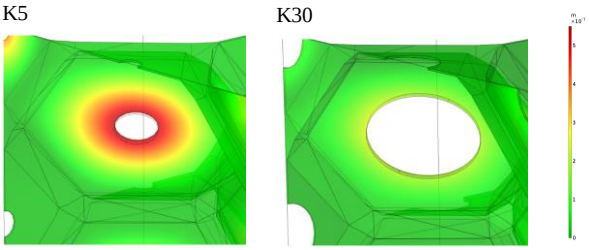

Figure 13. Contour plot of the displacement at time of maximum pressure on one hexagonal face of K5 (left column) and K30 (right column).

Conclusions

This paper shows how COMSOL Multiphysics® Modeling Software can be used to study the wave propagation problem in porous PU foams. Computational fluid dynamic has been used to predict foam permeability *k* through a 2D axial-symmetric reference model and a Kelvin foam model with regular cell hole sizes. The main factors which influence the permeability are size and cell hole area; indeed, increasing the opening ratio of the cell, the static permeability increases.

The coupling between air- and structure-borne wave propagation has been analysed to study the effect of cell face membranes. The bending of the thin membranes increases the fluid flow with an effect similar to have a larger cell opening. Then, velocity streamlines become less tortuous, the airflow resistance decreases and the static permeability increases. These effects decrease in the high frequency range, where the viscous dissipation decreases and the drag that the solid structure exerts on the fluid is dominated by inertia effects.

References

1. D. Randall, S. Lee, The Polyurethanes Handbook, London: Wiley, (2002);
2. M.T. Hoang, C. Perrot, Solid films and transports in cellular foams, *Journal of applied physics*, **112**, (2012);
3. F. Chevillotte, C. Perrot, E. Guillon. A direct link between microstructure and acoustical macro-behavior of real double porosity foams, *Journal of the Acoustical Society of America*, **134**, 4681-4690 (2013);
4. C. Zwikker,, C. W. Kosten, Sound Absorbing Materials, Elsevier Publishing Company, New York, (1949);

5. J.F. Allard, *Propagation of sound in porous media: modeling of sound absorbing materials*. Chapman and Hall, London (1993);

6. D.K. Wilson, Relaxation-matched modeling of propagation through porous media, including fractal pore structure, *The Journal of the Acoustical Society of America*, **94**, 1136-1145, (1993);

7. K. Gao, J.A.W. van Dommelen, M.G.D. Geers, Microstructure characterization and homogenization of acoustic polyurethane foams: measurements and simulations, *International Journal of Solids and Structures*, **100**, 536-546 (2016);

8. M. Brennan, J. Vandenbroeck, J. Peters, Using 3D computational solid and fluid mechanics to study the influence of foam cell microstructure and polymer viscoelasticity on the sound-absorbing behavior of polyurethane foams, *2nd International ATZ Conference: Automotive Acoustics Conference*, (2013);

9. N. Kino, G. Nakano, Y. Suzuki, Non-acoustical and acoustical properties of reticulated and partially reticulated polyurethane foams, *Applied Acoustic*, 73, 95-108 (2012);

10. M.A.Biot, Theory of propagation of elastic waves in a fluid-saturated porous solid. I. low-frequency range, *The Journal of the Acoustical Society of America*, **28**, 168–178 (1956). W. Thomson (Lord Kelvin): On the division of space with minimum partitional area. Philosophical Magazine, **24,** 151 (1887);

11. COMSOL® Multiphysics, User's Guide, version 5.3, 2017;

12. G.A. Holzapfel, *Nonlinear solid mechanics*, J. Wiley & Sons, New York, 2000;

13. A.N. Gent, K.C. Rusch, Viscoelastic behaviour of open cell foams, *Rubber Chemistry and Technology*, **39**, 389-396 (1966);

14. L. Boeckx, M. Brennan, K. Verniers, J. Vandenbroeck, A numerical scheme for investigating the influence of the three dimensional geometrical features of porous polymeric foam on its sound absorbing behaviour, *ACTA Acustica United with Acoustica*, **96**, 239-246, (2010);

15. G. Fitzgerald, I. Lyn, N.J. Mills, Airflow through polyurethane foams with near-circular cell-face holes, *Journal of Cellular Plastic*, **40**, 89-110 (2004);

16. N.J. Mills, The wet Kelvin model for air flow through open-cell polyurethane foams, *Journal of Materials Science*, **40**, 5845-5851 (2005).